LIMNOLOGY
and
OCEANOGRAPHY: METHODS

ASLO

Limnol. Oceanogr.: Methods 20, 2022, 350–360

doi: 10.1002/lom3.10491

The detection of bacterial exometabolites in marine dissolved organic matter through ultrahigh-resolution mass spectrometry

Sarah K. Bercovici [1]*, **Thorsten Dittmar,** [1,2] **Jutta Niggemann** [1]

[1]Institute for Chemistry and Biology of the Marine Environment, University of Oldenburg, Oldenburg, Germany
[2]Helmholtz Institute for Functional Marine Biodiversity (HIFMB), University of Oldenburg, Oldenburg, Germany

Abstract

Bacteria play a key role in sustaining the chemodiversity of marine dissolved organic matter (DOM), yet there is limited direct evidence of a major contribution of bacterial exometabolites to the DOM pool. This study tests whether molecular formulae of intact exometabolites can be detected in natural DOM via untargeted Fourier-transform ion cyclotron resonance mass spectrometry (FT-ICR-MS). We analyzed a series of quantitative mixtures of solid-phase extracted DOM from the deep ocean, of a natural microbial community and selected model strains of marine bacteria. Under standard instrument settings (200 broadband scans, mass range 92–1000 Da), 77% of molecular formulae were shared between the mesocosm and marine DOM. However, there was < 10% overlap between pure bacterial exometabolome with marine DOM, and in mixing ratios closest to mimicking natural environments (1% bacterial DOM, 99% marine DOM), only 4% of the unique bacterial exometabolites remained detectable. Further experiments with the bacterial exometabolome DOM mixtures using enhanced instrument settings resulted in increased detection of the exometabolites at low concentrations. At 1000 and 10,000 accumulated scans, 23% and 29% of the unique molecular formulae were detectable at low concentrations, respectively. Moreover, windowing a specific mass range encompassing a representative fraction of exometabolites tripled the number of unique detected formulae at low concentrations. Routine FT-ICR-MS settings are thus not always sufficient to distinguish bacterial exometabolome patterns from a seawater DOM background. To observe these patterns at higher sensitivity, we recommend a high scan number coupled with windowing a characteristic region of the molecular fingerprint.

Marine dissolved organic matter (DOM) is a complex mixture of molecules, consisting of hundreds of thousands of distinct compounds (Zark et al. 2017). One potential contributing factor to this high diversity is the exometabolome of marine bacteria. Even when provided a simple substrate, bacteria can produce a whole suite of highly diverse exometabolites (Lechtenfeld et al. 2015; Wienhausen et al. 2017; Noriega-Ortega et al. 2019). For instance, within exometabolites from selected model strains of the *Roseobacter* group, thousands of molecular masses of intact compounds were detected, showing that bacteria produce molecular diversity rivaling or even exceeding that of marine DOM (Noriega-Ortega et al. 2019). There is substantial evidence for the contribution of bacteria in producing and sustaining DOM diversity (Osterholz et al. 2015; Noriega-Ortega et al. 2019). Moreover, microbial products, such as D and L- enantiomers of amino acids, have been detected in seawater (McCarthy et al. 1998; Dittmar et al. 2001; Benner and Kaiser 2003).

Most molecular analytical techniques use chemical fragmentation to assess the building blocks of large macromolecules (Mopper et al. 2007) or target a small fraction of individual compounds in seawater (Kujawinski 2011). In metabolomics, these targeted studies are important for the detection and analysis of specific metabolites in the natural environment. However, untargeted studies can distinguish molecular fingerprints between environmental samples and discover new biomarkers through the simultaneous measurement of many metabolites (Alonso et al. 2015). These analyses typically use high-resolution mass spectrometry and generate large amounts of complex data.

Mass spectrometry acquires spectral data in the form of a mass-to-charge ratio (m/z) and a relative intensity of molecules within the ionized analyte. Electrospray ionization (ESI; Fenn et al. 1989) is one of the most common ionization

*Correspondence: sarah.bercovici@uni-oldenburg.de

methods in mass spectrometry. During the electrospray process, the loss or gain of a proton ionizes analyte molecules without destroying them, allowing for their intact detection (Fenn et al. 1989). Numerous studies in various fields (environmental, pharmaceutical, toxicology, medical) use ESI due to its ease of use, fast sample time, low solvent consumption, and ability to be used for diverse analytes with large polarity and size ranges (Mallet et al. 2004). However, the ESI signal can be affected by flow instability, background noise, mobile phase interferences, and ion competition between the droplets. These phenomena can suppress or enhance certain ions and have an established effect on both targeted and untargeted analyses (Ghosson et al. 2021). Moreover, past studies that use mass spectrometry to assess biomarkers, metabolites, pharmaceuticals, and environmental contaminants report concerns with ionization and matrix effects associated with ESI (Avery 2002; Matuszewski et al. 2003; Mei et al. 2003; Mallet et al. 2004; Rowland et al. 2014). When detecting an analyte in a sample with a high concentration of extraneous material, purification techniques through extraction or separation chromatography can reduce ion suppression and improve the signal (Annesley 2003). However, those studies are most often targeted analyses to look for specific compounds, such as known biomarkers or contaminants. In untargeted studies, complete separation of all individual constituents is most often impossible (Kang et al. 2007; Remane et al. 2010; Yan and Kaiser 2018). These matrix effects would likely influence untargeted analyses of marine DOM and marine bacterial metabolite samples. In any case, untargeted mass spectrometry analyses have used continuous accumulation of selective ions (CASI; hereafter referred to as windowing) and longer ion accumulation time to provide additional, important information on DOM (Petras et al. 2017). For instance, structural information can be inferred (Witt et al. 2009; Leyva et al. 2022) and the number of formulae that can be assigned to peaks increases by $\sim$ 40% (Sleighter et al. 2009; Cao et al. 2016).

The aim of this study was the establishment of a non-targeted, holistic approach on a molecular formula-level to broaden the analytical window as much as possible. The approach should allow for routine and fast screening of exometabolites in DOM samples extracted from seawater. The time-consuming and selective quantitative determination of individual microbial exometabolites in seawater was not in the focus of our study. Instead, this study focused on identifying and distinguishing specific fingerprints and patterns of bacterial metabolites from a seawater background. We used Fourier transform ion cyclotron resonance mass spectrometry (FT-ICR-MS) to assess the detection of bacterial exometabolites in seawater. Due to the ultra-high mass resolution of FT-ICR-MS, the molecular masses of thousands of individual compounds can be detected at high sensitivity within a single sample; it is thus a valuable tool for non-targeted and global characterization of the molecular composition of complex organic mixtures such as microbial exometabolomes and marine DOM (Sleighter et al. 2014). To further enhance analytical sensitivity of FT-ICR-MS, we collected up to 10,000 broadband mass spectra per sample and used CASI over a specific mass range (windowing).

Materials and procedures

DOM origin

Three types of DOM were used in this analysis: a marine DOM representative from the mesopelagic Pacific Ocean (collected from the Natural Energy Laboratory of Hawaii Authority in 2009; Green et al. 2014), a marine mesocosm DOM sample collected from a 3-yr experiment involving a natural seawater inoculum (Osterholz et al. 2015) and a bacterial exometabolome from *Phaeobacter inhibens* (GenBank: CP002976.1; Noriega-Ortega et al. 2019), a representative member of the *Roseobacter* group. Marine bacteria of the *Roseobacter* group are ubiquitous in the ocean and abundant during phytoplankton blooms (Buchan et al. 2014). Their exometabolomes contain thousands of molecular formulae and potentially contribute to the chemodiversity of marine DOM (Noriega-Ortega et al. 2019).

SPE-DOM extraction and DOC quantification

Samples for the mesocosm, exometabolome, and marine DOM were desalted and concentrated with PPL cartridges as described in Osterholz et al. (2015), Noriega-Ortega et al. (2019), and Green et al. (2014), respectively, following the method introduced by Dittmar et al. (2008). All extracts were stored at -20°C until FT-ICR-MS analysis. The extraction efficiency was determined through the concentration of extracted dissolved organic carbon, obtained from a Shimadzu TOC-VPCH total organic carbon analyzer equipped with an autosampler ASI-V via high-temperature catalytic combustion. The analyses were quality controlled using a DOC deep sea reference material (Hansell Biogeochemistry Laboratory, University of Miami; CV = 5%). The overall extraction efficiencies (calculated with DOC) for the mesocosm and exometabolome extracts were 35% and 31%, respectively (Osterholz et al. 2015; Noriega-Ortega et al. 2019). The extraction efficiency of the marine DOM sample was 61 $\pm$ 3% (Green et al. 2014).

Dilution experimental setup

In terms of carbon extracted, the following mixtures were prepared from the PPL extracts: 0%, 1%, 5%, 10%, 20%, 25%, 30%, 40%, 50%, 60%, 70%, 75%, 80%, 90%, 95%, 99%, and 100% of exometabolome DOM and 0%, 10%, 20%, 30%, 40%, 50%, 60%, 70%, 80%, 90%, and 100% of mesocosm DOM, respectively, each mixed with the extracted deep ocean reference DOM to a DOC concentration of 2.5 mg L^{-1}. These samples (17 mixtures of exometabolome with deep ocean DOM and 11 mixtures of mesocosm with deep ocean DOM) were analyzed on the FT-ICR-MS in routine settings with an autosampler (see below). Additionally, more concentrated solutions (5 mg C L^{-1}) of pure deep reference DOM, pure

exometabolome, and 1% exometabolome (99% deep reference water) were prepared for manual injections with 1000 or 10,000 broadband scans and a specific mass window (200–250 Da) with 1000 scans. The higher concentration enhances sensitivity, but requires manual quality control of the spectra, because for some samples, the ICR becomes overloaded at a DOC concentration of 5 mg L^{-1}. While the pure extracts were originally dissolved in methanol, the final solutions run on the FT-ICR-MS consisted of 50% methanol (LC–MS/MS grade, Sigma-Aldrich) and 50% ultrapure water.

DOM characterization by FT-ICR-MS

Ultrahigh-resolution mass spectrometry was performed on a Bruker Solarix XR 15 Tesla FT-ICR-MS (Bruker Daltonik GmbH) with ESI in negative ion mode, with a voltage of 4.5 kV. ESI negative ion mode was used in this case because this setting is typically used to measure marine DOM. The sample flow rate was 360 μL h^{-1}, the temperature was 200°C and the hexapole accumulation time was 0.65 ms. Mass spectra were accumulated with either 200, 1000, or 10,000 scans. The 200 scans were accumulated using an autosampler (CTC Analytics AG), while the 1000 and 10,000 scan samples were collected with manual injection. One sample with 200 accumulated scans takes 12 min to run and uses up 72 μL of sample (or 12.5 nmols C), with a rate of 6 μL min^{-1}. Samples with 1000 and 10,000 accumulated scans take 47 and 470 min (8 h) per sample and use up 282 μL (117 nmols C) and 2.8 mL (1.17 μmols C) of sample, respectively. Scans were accumulated in a mass window ranging from 92 to 1000 m/z. The spectra were calibrated as described in Riedel and Dittmar (2014) using an internal calibration list within the Bruker Daltonics Data Analysis software package. This list consists of 51 compounds present in the sample and covered the entire mass range from 92 to 1000 m/z. After calibration, the mass error was < 0.1 ppm. After calibration, the mass lists were processed using ICBM-OCEAN (Merder et al. 2020). ICBM-OCEAN uses a method detection limit (MDL) to account for noise and reduce systematic error to allow for a more precise formula attribution. The MDL calculation is described in detail in Riedel and Dittmar (2014) and Merder et al. (2020). Calculating the MDL is a more robust method to distinguish signal from noise than the traditionally used fixed signal-to-noise ratio, as it is based on a reproducible procedure and statistical significance analysis that removes noise peaks while keeping analyte peaks with low signal intensities (Riedel and Dittmar (2014)). Because of these analytical improvements associated with MDL, we strongly recommend using that approach instead of an S/N cutoff. The results of ICBM-OCEAN in this study were the "*Likeliest matches*" dataset, which provides the most likely molecular formulae based on a large homologous series network, isotope ratio verifications, and the smallest difference to the reference mass.

After data processing in ICBM-OCEAN, masses present in the blanks were considered contaminants and removed, and only masses up to 800 m/z were considered. Only those masses assigned molecular formulae were included in the analysis and isotopologues were removed from further consideration. All samples were run in triplicate and the mass spectra reported here are the mean of the replicates. Any peak whose height fell below the MDL when the triplicates were averaged was set to zero. The signal intensities were normalized by dividing the FT-ICR-MS signal intensity of each molecular mass by the total sum of intensities within each sample. We selected a window between m/z values of 200–250 m/z to isolate a range that includes most molecular formulae unique to the exometabolome. Data were analyzed and graphically represented using RStudio version 4.1 (R Core Team 2009–2021).

Distinguishing ESI suppression from MDL in the dilution series

To assess the extent to which ESI suppression plays a role in the detection of bacterial exometabolites in a marine DOM sample, we generated a dataset that considers only dilution and MDL, with no additional ion suppression from the ESI source. This simulated dataset was generated from the triplicate-averaged mass spectra from the pure bacterial exometabolome endmember and the pure marine endmember, and was calculated for each individual molecular formula as follows:

$$I_{n,simulated} = a \times I_{n,marine} + b \times I_{n,bacterial} \quad (1)$$

where a and b are the same dilution steps that add up to 100% (see previous sections) and $I_{n,marine}$ and $I_{n,bacterial}$ represent the FT-ICR-MS signal intensities (I) of each individual molecular formula (n) of the original marine and bacterial exometabolome endmembers, respectively. Then, to account for MDL, any peak height that fell below the MDL in the calculated dataset was set to zero. We therefore generated a dataset with this equation that would represent what the spectra would look like only affected by dilution and MDL. We compared this dataset with our observed data to identify any changes in detection due to factors beyond simple dilution and MDL.

Assessment

Distinguishing microbial DOM from marine DOM with automated routine settings

For the exometabolome, 44% of the detected masses were assigned unique formulae that followed the defined restrictions set for C, N, O, S, and P set in ICBM-OCEAN (Merder et al. 2020). For the mesocosm and deep seawater, 55% and 61% of the masses were assigned formulae, respectively. With routine settings, 1115 unique molecular formulae were detected in the exometabolome and 2456 unique to the deep-sea DOM endmembers. Only 111 were shared between the two DOM types (< 10% of total exometabolome formulae)

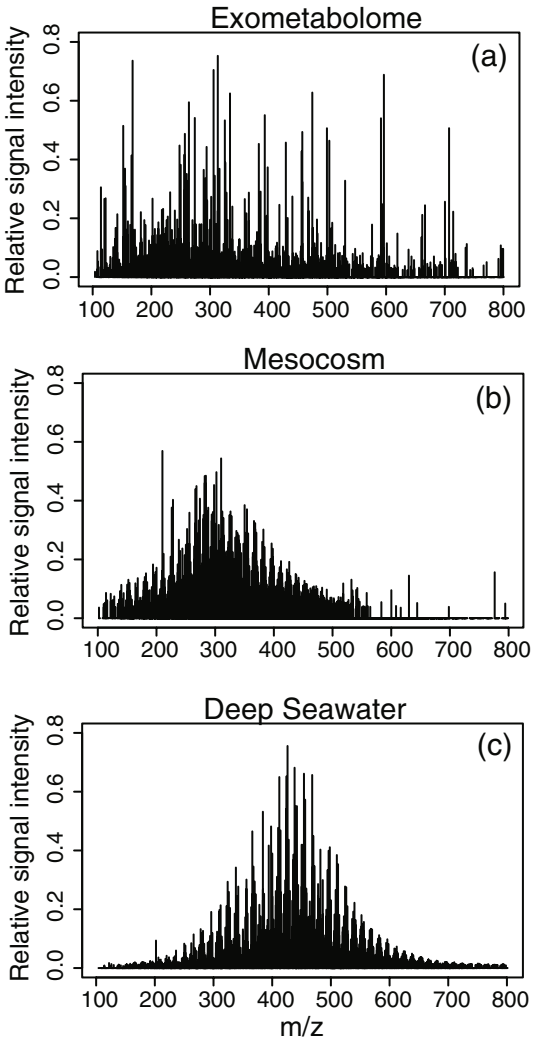

Fig. 1. Normalized FT-ICR-MS mass spectra of solid-phase extracted DOM from (**a**) *Roseobacter* exometabolome; (**b**) experimental mesocosm with natural microbial community; (**c**) natural deep seawater.

(Fig. 1; Table 1). As the mixing ratio of exometabolome to marine DOM decreased, most unique exometabolite peaks fell below the MDL. When the dilution mixture was 50% exometabolome, 29% of the unique exometabolome formulae were detected; when the mixture was 1% exometabolome, 7% of the unique formulae remained detectable, making up only 0.9% of the total relative peak abundance (Fig. 2). The mesocosm DOM (Fig. 1b) had a greater overlap with the deep seawater DOM; of the 1973 formulae detected in the mesocosm DOM, 77% were shared with deep seawater DOM and 23% were unique to the mesocosm (Table 1). At 50% mesocosm, 1847 of the 1973 original molecular formulae (94%) were detected. At 10% mesocosm, 1560 mesocosm formulae (79%) were detected; however, only 137 of those formulae were unique to the mesocosm, making up 0.6% of the relative abundance.

Detection of microbial DOM within a deep seawater background

To determine whether the microbial DOM signatures were selectively suppressed in relation to the deep seawater background, observations were compared to the simulated dataset described in Eq. 1. Detected signal intensities of mesocosm DOM fit well with the simulated intensities from our mixing model, suggesting that there was no additional ion suppression of mesocosm DOM beyond dilution and MDL constraints (Fig. 3). For the exometabolome DOM, slight ion suppression was observed in the presence of deep seawater DOM (Fig. 3): both the simulated relative abundance and total number of molecular formulae were typically higher than the observed relative abundance of the exometabolome. Overall, the observed deviations between expected and observed signal intensities were minor, indicating minor matrix effects and minor additional ion suppression due to mixing of different samples.

The total ion current (TIC), or the sum of all ions detected via FT-ICR-MS in a sample of exometabolome, mesocosm, or deep seawater DOM, also provides insights for why some molecular formulae are undetected beyond simple dilution (Fig. 3). If the TIC is normalized to the concentration of analyte (i.e., concentration of marine or microbial DOM) and there is no difference in ionization efficiency, there will be no change in the detector response, as was observed for both the deep seawater and the mesocosm (Fig. 3f). However, there was a linear change in the normalized TIC of the exometabolome, implying a reduced detector response of exometabolites when in the presence of marine DOM (Fig. 3c). Furthermore, the detector response for deep seawater is an order of magnitude greater than that of exometabolome DOM. Such a large difference in detector response is not evident for the mesocosm DOM sample, which showed no difference in ionization efficiency when compared to deep seawater.

Chemical characteristics of detected microbial DOM along the dilution series

There were limited notable changes in the chemical composition of detected/observed DOM for either type of microbial DOM when diluted (Fig. 4). The distribution of molecular masses and indices, and chemical ratios remained largely the same. However, lower molecular weight material was preferentially detected at low percentages of bacterial exometabolome and mesocosm (Fig. 4a,d). There are still marked differences between the mesocosm and marine DOM (Osterholz et al. 2015), but due to the high peak overlap, there is less ion suppression of the mesocosm and instead just loss in detection due to dilution (Fig. 3d). Because bacterial exometabolites in our DOM samples are likely affected by some ion suppression due to the ESI (Fig. 3c), in the following sections, we discuss possible steps to enhance their detection through increased scan numbers and windowing.

Table 1. Unique and shared exometabolome and mesocosm molecular formulae with marine DOM for samples run at 200 scans, and unique and shared formulae for the exometabolome run at 1000 (both broadband and windowed) and 10,000 scans.

	Total number of molecular formulae	Number of formulae overlapping with marine DOM	Unique microbial molecular formulae	Remaining unique microbial formulae*
200 scans				
Exometabolome	1226	111	1115	83 (7%)
Mesocosm	1973	1514	459	137 (30%)
1000 scans				
Exometabolome	1774	519	1255	289 (23%)
Windowed exometabolome (200–250 m/z)	837	183	654	176 (27%)
10,000 scans				
Exometabolome	11,610	5834	5776	1668 (29%)

*Unique molecular formulae remaining at the lowest concentration of microbial DOM (1% and 10% for the exometabolome and mesocosm, respectively).

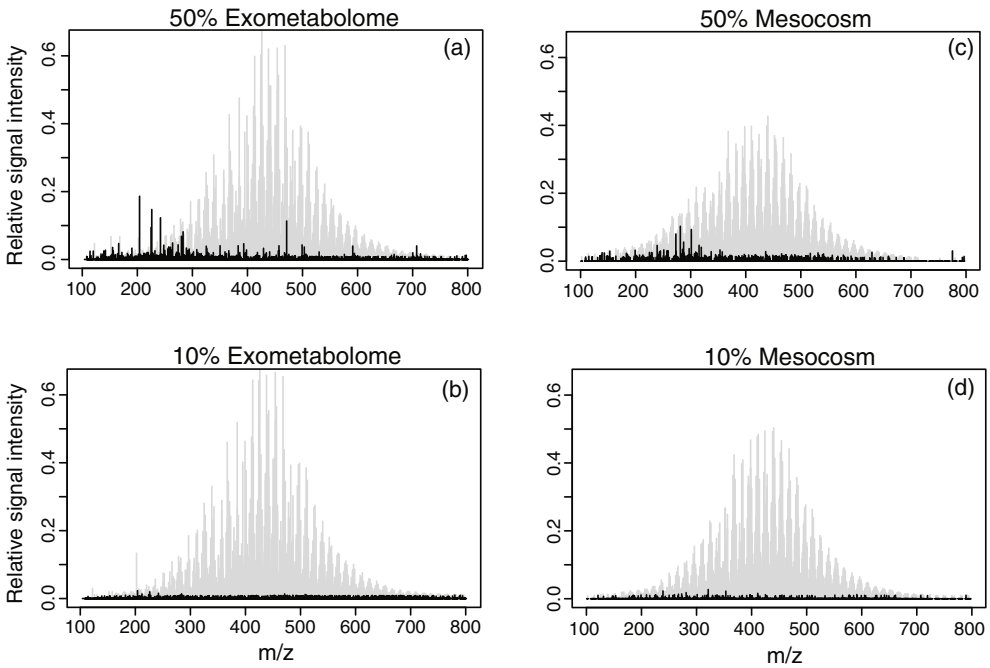

Fig. 2. Normalized FT-ICR-MS mass spectra of (**a**) 50% exometabolome mixed with 50% marine DOM; (**b**) 10% exometabolome mixed with 90% marine DOM; (**c**) 50% mesocosm mixed with 50% marine DOM; (**d**) 10% mesocosm mixed with 90% marine DOM. The gray background depicts the total spectrum of the mixture, while the black represents just those peaks unique to the microbial DOM.

Enhanced detection through increased scan numbers: 1000 and 10,000 scans

To assess improved settings for the detection of the exometabolome mixed with marine DOM, mass spectra consisting of 1000 and 10,000 accumulated scans of pure exometabolome, pure marine DOM and 1% exometabolome were obtained. We chose the 1% mixture to represent a sample that would more closely reflect the natural environment. An increase in scans allows for both an increased resolution and TIC. However, it also takes more time and more sample volume. While the 200-scan routine samples only take 12 min to run, and use up $\sim$ 70 μL of sample, the 1000 and 10,000 scan samples take 47 and 470 min (8 h) per sample, and use up 282 μL and 2.8 mL of sample, respectively. In the 1000-scan spectrum of pure exometabolome, there were 1774 identified molecular formulae, with 1255 (71%) of

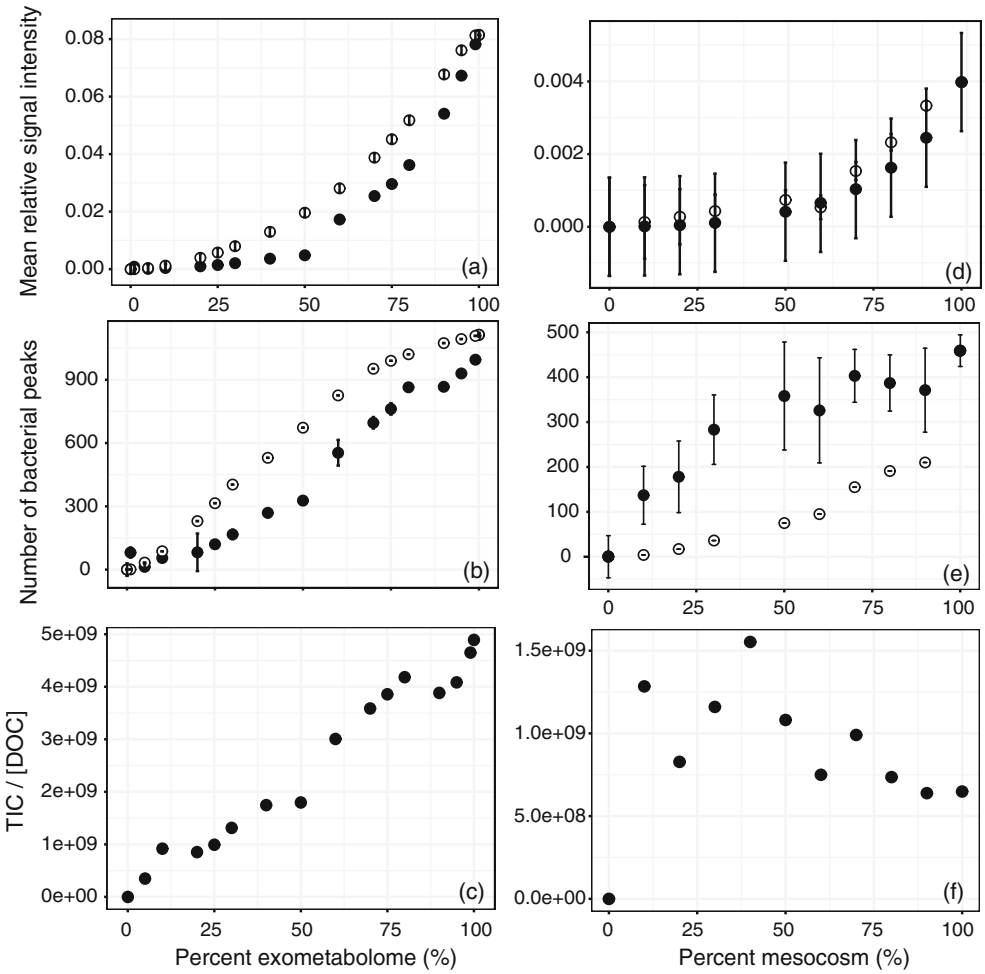

Fig. 3. Total relative peak abundance (**a**, **d**), number of unique detected formulae (**b**, **e**), and normalized TIC (**c**, **f**) of the unique exometabolome (left panels) and mesocosm (right panels) molecular formulae, respectively. Black dots represent observed data and white circles represent the simulated data based on only mixing and MDL. The error bars represent the error based on triplicate measurements for the observed data; for the modeled data, the error bars are the propagated error of the triplicates of the model endmembers.

them unique to the exometabolome (Table 1). In the 10,000-scan exometabolome sample, there were 11,610 formulae, with 5834 (50%) unique to the exometabolome (Table 1). In the 1000- and 10,000-scan spectra, 29% and 50% of exometabolome formulae were shared with marine DOM, respectively, suggesting that mass spectra with more accumulated scans contained more shared formulae between deep seawater DOM and the pure bacterial exometabolome.

In the 1% exometabolome sample at 1000 and 10,000 scans, 289 and 1668 (23 and 29%) of the unique exometabolome formulae remained detected, respectively (Table 1). These results show that a greater number of scans allows for greater detection of molecular formulae unique to a bacterial exometabolome when present at low concentrations. However, even at 10,000 scans, not all the molecular formulae present in the pure exometabolome were detected in the 1% sample, suggesting that these techniques providing higher resolution and signal to noise ratios will still not provide a complete representation of all bacterial exometabolites present in the marine environment. Overall, broadband scanning may not enhance the signal-to-noise ratio to sufficiently detect most bacterial metabolites in seawater. Instead, windowing a specific m/z range could provide further information that is not achievable with broadband scanning.

Windowed scans

An alternative approach to increase the detection of bacterial exometabolites is to use windowed scanning, which targets a specific m/z range. In this approach, we collected 1000 windowed scans of the pure and 1% exometabolome samples to determine if there was improved detection of unique formulae. A window between m/z values of 200–250 m/z was selected, as this range encompasses a large portion of molecular formulae unique to the exometabolome (> 55%; Fig. 1a).

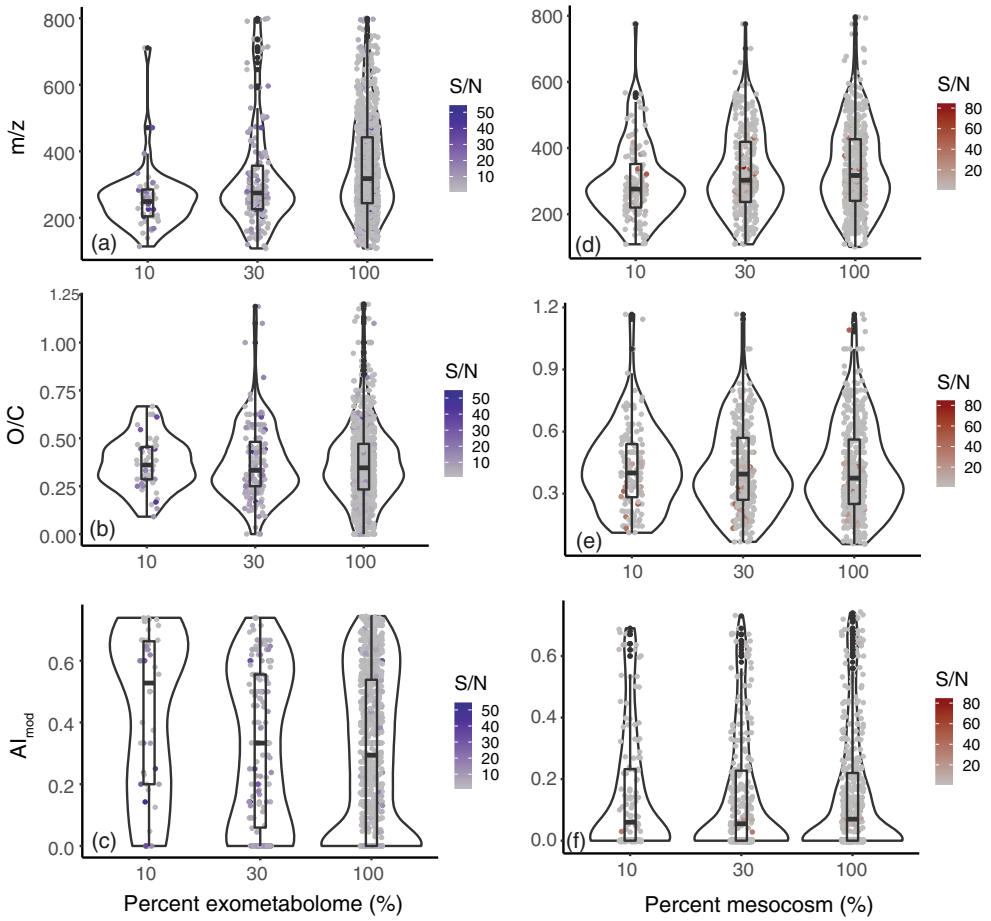

Fig. 4. Violin plots of the distribution of m/z, oxygen-to-carbon ratio (O/C), and aromaticity index (AI_{mod}) for 10%, 30%, and 100% exometabolome (**a**, **b**, **c**) and mesocosm (**d**, **e**, **f**), respectively; color bars represent the signal to MDL ratio of each molecular formulae. Violin plots use kernel density and box plots to depict the probability density, average and standard deviation of the data.

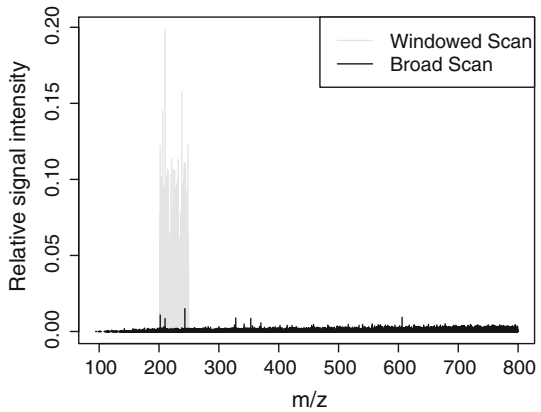

Fig. 5. Windowed (gray) and broadband (black) mass spectra (1000 scans) between 200 and 250 m/z of unique exometabolome peaks within a 1% exometabolome (99% deep seawater) solution.

Furthermore, this range only contains 93 formulae (2%) unique to the marine DOM, as most of the m/z distribution of marine DOM ranges between 300 and 800 (Fig. 1c).

In the windowed pure exometabolome spectrum, 837 molecular formulae were detected, with 654 (72%) of them unique to the exometabolome (Table 1; Fig. 5). In contrast, 331 unique exometabolome formulae were detected in the broadband 1000-scan sample. In the 1% exometabolome windowed sample, 176 (27%) of those unique molecular formulae were detected, making up 12% of the relative abundance. In the same 200–250 m/z range of the 1% exometabolome broadband scan sample, only 55 peaks (17%) of the original unique exometabolome formulae were detected, comprising 0.1% of the relative abundance (Fig. 5). Overall, windowing nearly doubled the number of detected unique exometabolome molecular formulae in the pure exometabolome sample; in the 1% exometabolome sample, the number of detected peaks tripled.

Discussion

In this study, we tested whether molecular formulae of intact exometabolites can be detected in marine DOM. The extraction efficiencies of the exometabolome and mesocosm were relatively low (31% and 35%, respectively) as compared

to the marine DOM, suggesting that the bacterial DOM is less efficient at binding to the PPL cartridge. Generally, aromatic compounds that are neutral during PPL extraction have a high retention, while smaller, charged molecules with less aromaticity (such as certain amino acids and peptides) are not as efficiently extracted by PPL (Johnson et al. 2017). As bacterial DOM is typically enriched in these smaller, more polar metabolites as compared to marine DOM, we are likely missing an important component of that DOM. In any case, SPE encompasses a representative fraction of both microbial and marine DOM, which is reproducible and clearly defined by its physico-chemical properties. Moreover, for the exometabolome DOM, some ion suppression was observed in the presence of deep seawater DOM (Fig. 3a). The detectable molecular formulae in pure exometabolome DOM have a lower response factor compared to more processed microbial DOM and ultimately seawater DOM.

The results of this study suggest that in negative ion mode, pure exometabolites do not ionize as efficiently as more processed DOM, even though they are all polar, water soluble, and PPL extracted. Positive ion mode may improve the detection of bacterial metabolites (as observed in the method conducted in Kujawinski et al. (2016)). Longnecker et al. (2015) applied both positive and negative mode on diatom exudates and detected up to three times more features in positive mode. In fact, positive and negative mode are each more efficient at characterizing different components of DOM, and so a combination of the two modes may allow for a more complete detection of all possible metabolites (Ohno et al. 2016). However, DOM processed by a diverse microbial community, such as the mesocosm DOM in this experiment, more closely resembles marine DOM, and thus had more efficient ionization (Romano et al. 2014; Osterholz et al. 2015). In this experiment, the majority of the mesocosm formulae were shared with deep seawater (Table 1). Continuous bacterial processing, such as that observed in the mesocosm, diversifies DOM, which in turn would increase its ionizability and detector response (Fig. 3d–f). Less-processed bacterial DOM, such as the bacterial exometabolome, appears to exhibit less ionization when in the presence of the matrix of marine DOM (Fig. 3a–c). These results indicate a minor matrix effect for the bacterial exometabolome. As with FT-ICR-MS, we do not separate our exometabolome chromatographically before the sample enters the ESI chamber, ion crowding may lead to suppression that would be limited if a chromatographic separation were conducted beforehand.

When considering chemical changes of detected microbial DOM, lower molecular weight material was preferentially detected at low percentages of bacterial exometabolome (Fig. 4a), suggesting that the m/z distribution of microbial DOM within a seawater sample may not represent its full size range. Other studies using FT-ICR-MS likewise reported that ion suppression due to the ESI preferentially suppresses larger material (Rowland et al. 2014). While it is possible to account for relative matrix effects between metabolites, it is difficult when the two sample matrixes are extremely divergent (Böttcher et al. 2007). Moreover, a mixture of DOM from different sources may lead to differences in analyte signal on the FT-ICR-MS (Gan et al. 2021). In the case of this study, the bacterial exometabolite matrix is markedly different than the marine DOM matrix (Fig. 1; Table 1), and both ion suppression due to the ESI and differences in ionization efficiency due to structural variations between the microbial and marine DOM may play roles in why we observe relative suppression of the exometabolites.

Increasing the number of scans or increasing the analyte concentration improves the TIC and mass resolution on the FT-ICR-MS (Marshall et al. 1998). However, the resolution will also increase for the marine DOM background and increasing the DOC concentration of the analyte will saturate the ion cyclotron resonance (ICR) detection cell (Schermann 2008). Moreover, the amount of time required to run one sample becomes a constraint. While the 200 scan samples only take 12 min, the 10,000 scan samples take a full workday. In comparison, an LC–MS method using chromatographic separation and subsequent analysis of cultured diatom DOM takes approximately 33 min (Longnecker and Kujawinski 2017). In the windowing approach, only a fraction of all ionized molecules is transferred to the ICR detection cell, thus avoiding saturation of the cell. Therefore, windowing increases sensitivity of the analysis because much higher concentrations can be used without overloading the cell.

Windowing detects a larger proportion of unique exometabolites at low concentrations that were not detectable even at 10,000 scans. This technique would not necessarily work; however, if there were greater overlap between the bacterial and marine molecular formulae, since all signals in the window range would be enhanced. Windowing would thus be the most effective if the bacterial DOM had clear separation from marine DOM. As such, unique characteristics of bacterial DOM that distinguish it from marine DOM must first be assessed with broadband scanning. If that prerequisite is met, then windowing may provide more detailed information on bacterial exometabolites within marine DOM.

Overall, the ability to identify specific biological exometabolites within marine DOM is important to fully understand its vast complexity, and untargeted ultrahigh-resolution mass spectrometry has the potential to provide important insights. As a DOM sample contains > 200,000 compounds (Zark et al. 2017), there are thousands of unidentified molecules present in marine and bacterial DOM. However, past work using untargeted LC–MS/MS of marine DOM reported that only 1% of detectable DOM compounds can be structurally or molecularly identified (Petras et al. 2017). Moreover, our study suggests that their detection may have limitations when using routine settings in FT-ICR-MS. The concentration of individual compounds in marine DOM is likely in the picomolar range (Dittmar 2015), so the contribution of pure bacterial

exometabolome in an environmental sample would be miniscule. Bacterial exometabolites would more likely be detectable with FT-ICR-MS during a DOM production event such as a phytoplankton bloom, when bacteria are provided fresh material to metabolize. However, even during one of these events in the North Atlantic, bacterially produced vitamin B12 only reached 4 pM (Panzeca et al. 2009). Pure cultures, such as the exometabolome presented in this study, have an excess of carbon that would likely surmount what is observed in the natural environment. Furthermore, as the exometabolome endmember measured here is an endmember from a pure *P. inhibens* culture (Noriega-Ortega et al. 2019), this exometabolome endmember does not fully represent the DOM that would be produced by the natural microbial assembly in the marine environment. Moreover, previous studies on the Roseobacter exometabolome showed the vast diversity of exometabolomes of closely related strains produced under different growth conditions (substrate) and growth stages (Wienhausen et al. 2017; Noriega-Ortega et al. 2019). In any case, we were interested in the potential detection of specific bacterial exometabolites/fingerprints, and here, the chosen well-defined exometabolome of *P. inhibens* served as a model exometabolome. We also included the microbial DOM from the mesocosm study, integrating a multitude of different exometabolomes of changing microbial communities, which may provide a more accurate representation of a natural microbial assembly.

Based on the results of this study, our method recommendations to detect the environmental occurrence of exometabolites within marine DOM would be to run samples initially with broadband settings at a higher number of scans (like the 1000 or 10,000 scan runs in this experiment). Then, if there is an m/z range where these exometabolites can be clearly distinguished from the seawater DOM background, windowing that characteristic mass range may increase the detection of exometabolites. However, measuring over only a selected mass range would require more instrument time and more sample material than in broadband mode. Therefore, this technique is best suited when there is sufficient sample material and capabilities to make measurements with high scan numbers on the FT-ICR-MS. Moreover, future work that uses positive ion mode or both negative and positive ion modes (Kujawinski et al. 2016; Ohno et al. 2016) may provide more details about bacterial exometabolites. Using LC–MS/MS to determine structural features unique to the bacterial DOM may further enhance the detection of bacterial metabolites within marine DOM. If sample amount is not a limitation in an experiment, it would be worthwhile to increase the number of windowed regions to determine whether there are multiple possible regions that enhance and illustrate the exometabolome fingerprint. Nevertheless, applying the recommended approach to even a few select samples would provide novel information on the origin, turnover, and dynamics of unidentified exometabolites in aquatic and marine environments.

Data availability statement

All data described in this work are available upon request from Sarah K. Bercovici.

References

Alonso, A., S. Marsal, and A. Julià. 2015. Analytical methods in untargeted metabolomics: State of the art in 2015. Front. Bioeng. Biotechnol. **3**: 23. doi:10.3389/fbioe.2015.00023

Annesley, T. M. 2003. Ion suppression in mass spectrometry. Clin. Chem. **49**: 1041–1044. doi:10.1373/49.7.1041

Avery, M. J. 2002. Quantitative characterization of differential ion suppression on liquid chromatography/atmospheric pressure ionization mass spectrometric bioanalytical methods. Rapid Commun. Mass Spectrom. **17**: 197–201. doi:10.1002/rcm.895

Benner, R., and K. Kaiser. 2003. Abundance of amino sugars and peptidoglycan in marine particulate and dissolved organic matter. Limnol. Oceanogr. **1**: 118–128. doi:10.4319/lo.2003.48.1.0118

Böttcher, C., E. V. Roepenack-Lahaye, E. Willscher, D. Scheel, and S. Clemens. 2007. Evaluation of matrix effects in metabolite profiling based on capillary liquid chromatography electrospray ionization quadrupole time-of-flight mass spectrometry. Anal. Chem. **79**: 1507–1151. doi:10.1021/ac061037q

Buchan, A., G. R. LeCleir, C. A. Gulvik, and J. M. Gonzalez. 2014. Master recyclers: Features and functions of bacteria associated with phytoplankton blooms. Nat. Rev. Microbiol. **12**: 686–698. doi:10.1038/nrmicro3326

Cao, D., J. Lv, F. Geng, Z. Rao, H. Niu, Y. Shi, Y. Cai, and Y. Kang. 2016. Ion accumulation time dependent molecular characterization of natural organic matter using electrospray ionization-Fourier transform ion cyclotron resonance mass spectrometry. Anal. Chem. **88**: 12210–12218. doi:10.1021/acs.analchem.6b03198

Dittmar, T. 2015. Reasons behind the long-term stability of dissolved organic matter, p. 369–388. *In* D. A. Hansell and C. A. Carlson [eds.], Biogeochemistry of marine dissolved organic matter. Elsevier Inc.. doi:10.1016/B978-0-12-405940-5.00007-8

Dittmar, T., H. P. Fitznar, and G. Kattner. 2001. Origin and biogeochemical cycling of organic nitrogen in the eastern Arctic Ocean as evident from D- and L-amino acids. Geochim. Cosmochim. Acta **65**: 4103–4114. doi:10.1016/S0016-7037(01)00688-3

Dittmar, T., B. Koch, N. Hertkorn, and G. Kattner. 2008. A simple and efficient method for the solid-phase extraction of dissolved organic matter (SPE-DOM) from seawater. Limnol. Oceanogr: Methods. **6**: 230–235. doi:10.4319/lom.2008.6.230

Fenn, J. B., M. Mann, C. K. Meng, S. F. Wong, and C. M. Whitehouse. 1989. Electrospray ionization for mass

spectrometry of large biomolecules. Science **246**: 64–71. doi:10.1126/science.2675315

Gan, S., P. Guo, Y. Wu, and Y. Zhao. 2021. A novel method for unraveling the black box of dissolved organic matter in soils by FT-ICR-MS coupled with induction-based nanospray ionization. Environ. Sci. Technol. Lett. **8**: 356–361. doi:10.1021/acs.estlett.1c00095

Ghosson, H., Y. Guitton, A. Ben Jrad, C. Patil, D. Raviglione, M.-V. Salva, and C. Bertrand. 2021. Electrospray ionization and heterogeneous matrix effects in liquid chromatography/mass spectrometry based meta-metabolomics: A biomarker or a suppressed ion? Rapid Commun. Mass Spectrom. **35**: e8977. doi:10.1002/rcm.8977

Green, N. W., E. M. Perdue, G. R. Aiken, K. D. Butler, H. Chen, T. Dittmar, J. Niggemann, and A. Stubbins. 2014. An intercomparison of three methods for the large-scale isolation of oceanic dissolved organic matter. Mar. Chem. **161**: 14–19. doi:10.1016/j.marchem.2014.01.012

Johnson, W. M., M. C. Kido Soule, and E. B. Kujawinski. 2017. Extraction efficiency and quantification of dissolved metabolites in targeted marine metabolomics. Limnol. Oceanogr.: Methods **15**: 417–428. doi:10.1002/lom3.10181

Kang, J., L. A. Hick, and W. E. Price. 2007. Using calibration approaches to compensate for remaining matrix effects in quantitative liquid chromatography electrospray ionization multistage mass spectrometric analysis of phytoestrogens in aqueous environmental samples. Rapid Commun. Mass Spectrom. **21**: 4065–4072. doi:10.1002/rcm.3311

Kujawinski, E. 2011. The impact of microbial metabolism on marine dissolved organic matter. Ann. Rev. Mar. Sci. **3**: 567–599. doi:10.1146/annurev-marine-120308-081003

Kujawinski, E. B., K. Longnecker, K. L. Barott, R. J. M. Weber, and M. C. Kido Soule. 2016. Microbial community structure affects marine dissolved organic matter composition. Front. Mar. Sci. **3**: 45. doi:10.3389/fmars.2016.00045

Lechtenfeld, O. J., N. Hertkorn, Y. Shen, M. Witt, and R. Benner. 2015. Marine sequestration of carbon in bacterial metabolites. Nature Commun. **6**: 6711. doi:10.1038/ncomms7711

Leyva, D., M. U. Tariq, R. Jaffé, F. Saeed, and F. Fernandez Lima. 2022. Unsupervised structural classification of dissolved organic matter based on fragmentation pathways. Environ. Sci. Technol. **56**: 1458–1468. doi:10.1021/acs.est.1c04726

Longnecker, K., and E. B. Kujawinski. 2017. Mining mass spectrometry data: Using new computational tools to find novel organic compounds in complex environmental mixtures. Org. Geochem. **110**: 92–99. doi:10.1016/j.orggeochem.2017.05.008

Longnecker, K., J. Futrelle, E. Coburn, M. C. Kido Soule, and E. B. Kujawinski. 2015. Environmental metabolomics: Databases and tools for data analysis. Mar. Chem. **177**: 366–373. doi:10.1016/j.marchem.2015.06.012

Mallet, C. R., Z. Lu, and J. R. Mazzeo. 2004. A study of ion suppression effects in electrospray ionization from mobile phase additives and solid-phase extracts. Rapid Commun. Mass Spectrom. **18**: 49–58. doi:10.1002/rcm.1276

Marshall, A. G., C. L. Hendrickson, and G. S. Jackson. 1998. Fourier transform ion cyclotron resonance mass spectrometry: A primer. Mass Spectrom. Rev. **17**: 1–35. doi:10.1002/(SICI)1098-2787(1998)17:1<1::AID-MAS1>3.0.CO;2-K

Matuszewski, B. K., M. L. Constanzer, and C. M. Chavez-Eng. 2003. Strategies for the assessment of matrix effect in quantitative bioanalytical methods based on HPLC−MS/MS. Anal. Chem. **75**: 3019–3030. doi:10.1021/ac020361s

McCarthy, M. D., J. I. Hedges, and R. Benner. 1998. Major bacterial contribution to dissolved organic nitrogen. Science **281**: 231–234. doi:10.1126/science.281.5374.231

Mei, H., Y. Hsieh, C. Nardo, X. Xu, S. Wang, K. Ng, and W. A. Korfmacher. 2003. Investigation of matrix effects in bioanalytical high-performance liquid chromatography/tandem mass spectrometric assays: Application to drug discovery. Rapid Commun. Mass Spectrom. **17**: 97–103. doi:10.1002/rcm.876

Merder, J., J. A. Freund, U. Feudel, J. Niggemann, G. Singer, and T. Dittmar. 2020. Improved mass accuracy and isotope confirmation through alignment of ultrahigh-resolution mass spectra of complex natural mixtures. Anal. Chem. **92**: 2558–2565. doi:10.1021/acs.analchem.9b04234

Mopper, K., A. Stubbins, J. D. Ritchie, H. M. Bialik, and P. G. Hatcher. 2007. Advanced instrumental approaches for characterization of marine dissolved organic matter: Extraction techniques, mass spectrometry, and nuclear magnetic resonance spectroscopy. Chem. Rev. **107**: 419–442. doi:10.1021/cr050359b

Noriega-Ortega, B. E., G. Wienhausen, A. Mentges, T. Dittmar, M. Simon, and J. Niggemann. 2019. Does the chemodiversity of bacterial exometabolomes sustain the chemodiversity of marine dissolved organic matter? Front. Microbiol. **10**: 215. doi:10.3389/fmicb.2019.00215

Ohno, T., R. L. Sleighter, and P. G. Hatcher. 2016. Comparative study of organic matter chemical characterization using negative and positive mode electrospray ionization ultrahigh-resolution mass spectrometry. Anal. Bioanal. Chem. **408**: 2497–2504. doi:10.1007/s00216-016-9346-x

Osterholz, H., J. Niggemann, H.-A. Giebel, M. Simon, and T. Dittmar. 2015. Inefficient microbial production of refractory dissolved organic matter in the ocean. Nature Commun. **6**: 7422. doi:10.1038/ncomms8422

Panzeca, C., A. J. Beck, A. Tovar-Sanchez, J. Segovia-Zavala, G. T. Taylor, C. J. Gobler, and S. A. Sañudo-Wilhelmy. 2009. Distributions of dissolved vitamin B12 and co in coastal and open-ocean environments. Estuar. Coast. Shelf Sci. **85**: 223–230. doi:10.1016/j.ecss.2009.08.016

Petras, D., I. Koester, R. Da Silva, B. M. Stephens, A. F. Haas, C. E. Nelson, L. W. Kelly, L. I. Aluwihare, and P. C. Dorrestein. 2017. High-resolution liquid chromatography

tandem mass spectrometry enables large scale molecular characterization of dissolved organic matter. Front. Mar. Sci. **4**: 405. doi:10.3389/fmars.2017.00405

Remane, D., D. K. Wissenbach, M. R. Meyer, and H. H. Maurer. 2010. Systematic investigation of ion suppression and enhancement effects of fourteen stable-isotope-labeled internal standards by their native analogues using atmospheric-pressure chemical ionization and electrospray ionization and the relevance for multi-analyte liquid chromatographic/mass spectrometric procedures. Rapid Commun. Mass Spectrom. **24, (7**: 859–867. doi:10.1002/rcm.4459

Riedel, T., and T. Dittmar. 2014. A method detection limit for the analysis of natural organic matter via Fourier transform ion cyclotron resonance mass spectrometry. Anal. Chem. **86**: 8376–8382. doi:10.1021/ac501946m

Romano, S., T. Dittmar, V. Bondarev, R. J. M. Weber, M. R. Viant, and H. N. Schulz-Vogt. 2014. Exo-metabolome of Pseudovibrio sp. FO-BEG1 analyzed by ultra-high resolution mass spectrometry and the effect of phosphate limitation. PLoS ONE **9**: e96038. doi:10.1371/journal.pone.0096038

Rowland, S. M., W. K. Robbins, Y. E. Corilo, A. G. Marshall, and R. P. Rodgers. 2014. Solid-phase extraction fractionation to extend the characterization of naphthenic acids in crude oil by electrospray ionization Fourier transform ion cyclotron resonance mass spectrometry. Energy Fuel **28**: 5043–5048. doi:10.1021/ef5015023

Schermann, J-P. Spectroscopy and modeling of biomolecular building blocks, 2008. 129–207, Elsevier, https://doi.org/10.1016/B978-0-444-52708-0.X5001-1

Sleighter, R. L., G. A. McKee, and P. G. Hatcher. 2009. Direct Fourier transform mass spectral analysis of natural waters with low dissolved organic matter. Org. Geochem. **40**: 119–125. doi:10.1016/j.orggeochem.2008.09.012

Sleighter, R. L., R. M. Cory, L. A. Kaplan, H. A. N. Abdulla, and P. G. Hatcher. 2014. A coupled geochemical and biogeochemical approach to characterize the bioreactivity of dissolved organic matter from a headwater stream. JGR Biogeosci. **119**: 1520–1537. doi:10.1002/2013JG002600

Wienhausen, G., B. E. Noriega-Ortega, J. Niggemann, T. Dittmar, and M. Simon. 2017. The exometabolome of two model strains of the Roseobacter group: A marketplace of microbial metabolites. Front. Microbiol. **8**: 1985. doi:10.3389/fmicb.2017.01985

Witt, M., J. Fuchser, and B. P. Koch. 2009. Fragmentation studies of fulvic acids using collision induced dissociation Fourier transform ion cyclotron resonance mass spectrometry. Anal. Chem. **81**: 2688–2694. doi:10.1021/ac802624s

Yan, G., and K. Kaiser. 2018. A rapid and sensitive method for the analysis of lignin phenols in environmental samples using ultra-high performance liquid chromatography-electrospray ionization-tandem mass spectrometry with multiple reaction monitoring. Anal. Chim. Acta **1023**: 74–80. doi:10.1016/j.aca.2018.03.054

Zark, M., J. Christoffers, and T. Dittmar. 2017. Molecular properties of deep-sea dissolved organic matter are predictable by the central limit theorem: Evidence from tandem FT-ICR-MS. Mar. Chem. **191**: 9–15. doi:10.1016/j.marchem.2017.02.005

Acknowledgments

The authors would like to thank Beatriz Noriega-Ortega and Gerrit Wienhausen for conducting the incubation experiments and obtaining the bacterial exometabolome DOM, and Helena Osterholz for the mesocosm DOM. They would also like to thank Helena Osterholz and Katrin Klaproth for their help with the FT-ICR-MS analyses and data interpretation. Funding was provided by Deutsche Forschungsgemeinschaft (DFG) within the Collaborative Research Center Roseobacter (TRR 51). Open Access funding enabled and organized by Projekt DEAL.

Submitted 31 December 2021
Revised 13 April 2022
Accepted 19 April 2022

Associate editor: Krista Longnecker